The Role of Slip in Turbulent Thermal Convection

Sai Ravi Gupta Polasanapalli[1,2,*] · Marten Klein[1,2] · Heiko Schmidt[1,2]

[1]Chair of Numerical Fluid and Gas Dynamics, Brandenburg University of Technology Cottbus-Senftenberg, Cottbus, Germany .

[*]**Contact:** sairavigupta.polasanapalli@b-tu.de

[2]Scientific Computing Lab, Energy Innovation Center, Brandenburg University of Technology Cottbus-Senftenberg, Cottbus, Germany.

Brandenburg University of Technology Cottbus - Senftenberg

Energie-Innovationszentrum Cottbus

Introduction

- **Functional surface coatings** enhance drag reduction, corrosion resistance, and wear protection while improving thermal and electrical insulation.
- **Hydrophobic** and **super-hydrophobic surfaces**, in particular, are widely used for drag reduction and self-cleaning in transport applications [1, 2].
- The **Navier slip** model is commonly used to characterize hydrophobic and super-hydrophobic surfaces [3].
- Functional coatings and textures can passively influence scalar transfer in technical flows by altering surface energy properties and alter the boundary conditions.
- **Fig. 1(a) and 1(b)** display the schematic domain setup and Navier-slip boundary condition implementation.

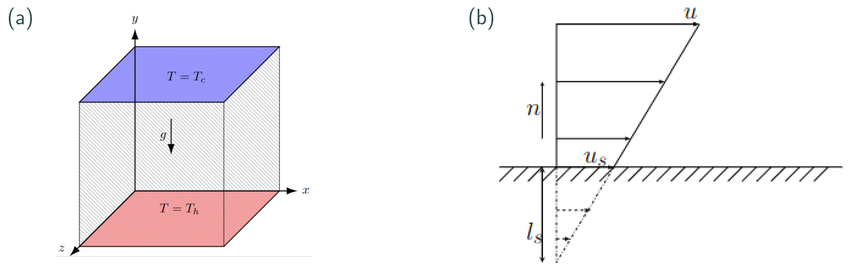

Figure 1: (a) Schematic diagram of the Rayleigh–Bénard set-up in the cubic cavity. (b) Schematic of the Navier-slip boundary condition using a slip velocity u_s and a slip length l_s.

Research Objectives

- **Investigate** the impact of **different surface boundary conditions** (no-slip, free-slip, finite-slip) on flow dynamics and heat transfer in turbulent Rayleigh-Bénard convection.
- Compare the effects of **horizontal vs. vertical wall boundary conditions** and **isotropic vs. anisotropic slip** on convective behavior.
- Analyze high-resolution 3D simulations (DNS) using the **off-lattice Boltzmann Method (OLBM)** at $Ra = 2 \times 10^6$, and 10^7 and $Pr = 0.786, 4.38$, and 10.
- Provide insights for optimizing heat transfer in engineering applications through tailored surface boundary conditions.

Off-Lattice Boltzmann Method (OLBM) in a Nutshell

- Uses **discrete-velocity Boltzmann equation** as governing equation to recover momentum and energy equations:

$$\frac{\partial f_k}{\partial t} + \mathbf{e_k}.\nabla f_k = -\frac{f_k - f_k^{eq}}{\tau_h} + F, \quad \text{for } k = 0, 1, 2, .., 26 \tag{1}$$

$$\frac{\partial g_k}{\partial t} + \hat{\mathbf{e}}_\mathbf{k}.\nabla g_k = -\frac{g_k - g_k^{eq}}{\tau_t}, \quad \text{for } k = 0, 1, 2, .., 6 \tag{2}$$

- The flow macroscopic properties are calculated as follows:

$$\rho(\mathbf{x}, t) = \sum_{k=0}^{26} f_k(\mathbf{x}, t), \;\; \rho\mathbf{V}(\mathbf{x}, t) = \sum_{k=0}^{26} f_k(\mathbf{x}, t).\mathbf{e_k}, \;\; T = \sum_{k=0}^{6} g_k(\mathbf{x}, t). \tag{3}$$

- Finite-difference based **off-lattice Boltzmann method (OLBM)** formulation is used [4].
- **Curvilinear Grids:** Handles complex geometries via body-fitted meshes.
- **High-Order Accuracy:** Employs second-order central difference schemes with 6th order filtering.
- **Efficiency:** OLBM reduces grid constraints compared to standard LBM while maintaining stability.

Thermal Convection in a Confinement with a Functional Wall

- Surface boundary conditions significantly alter both flow and thermal fields. Flow reversal behavior occurs in all configurations except the FS case, where free-slip boundary conditions are considered for all the walls.
- **Fig. 2(a)–(b)** present instantaneous isothermal contours for no-slip and free-slip surface conditions.
- **Fig. 3(a)–(c)** present time- and spanwise-averaged isotherms and streamlines, revealing temperature distributions and flow structures under different surface conditions. Four vortices are observed in the NS and FS-hori cases as (2, 2) 'vortex modes', while only a single vortex, (1, 1) vortex mode, is observed for the free-slip cases FS and FS-side.
- **Fig. 4(a)–(c)** show horizontal (x-z plane) averaged profiles of statistical quantities along the normalized vertical coordinate ($Y = y/H$) for varying velocity boundary conditions. Under free-slip boundary conditions, the flow velocity is larger, leading to a thinner thermal boundary layer compared to the no-slip case, where a steeper gradient near the walls and uniformity in the central region is prominent. The zero shear stress at the boundary in free-slip cases can lead to more intense turbulence, as the fluid near the walls experiences less resistance and can move more freely. Consequently, the TKE is generally higher for the FS case than the no-slip case.
- The heat transfer rate rises by 100% with free-slip conditions on all walls, by 60.11% with free-slip on horizontal walls only, and by 11.72% with free-slip on vertical side walls only for $Ra = 2 \times 10^6$ and $Pr = 4.38$. In cases with finite-slip boundaries, the heat transfer rate shows a slight increase and varying slip lengths have little impact.

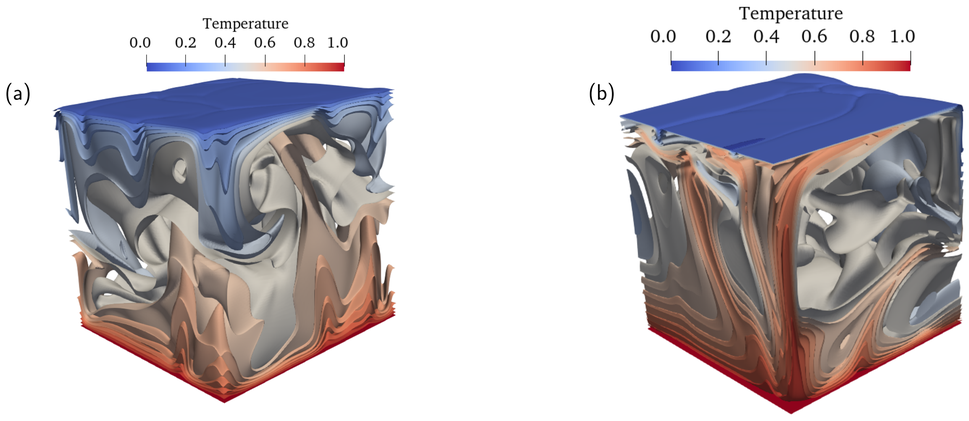

Figure 2: Instantaneous isothermal contours at $Ra = 1 \times 10^7$, $Pr = 4.38$ for (a) No-slip case, (b) Free-slip case.

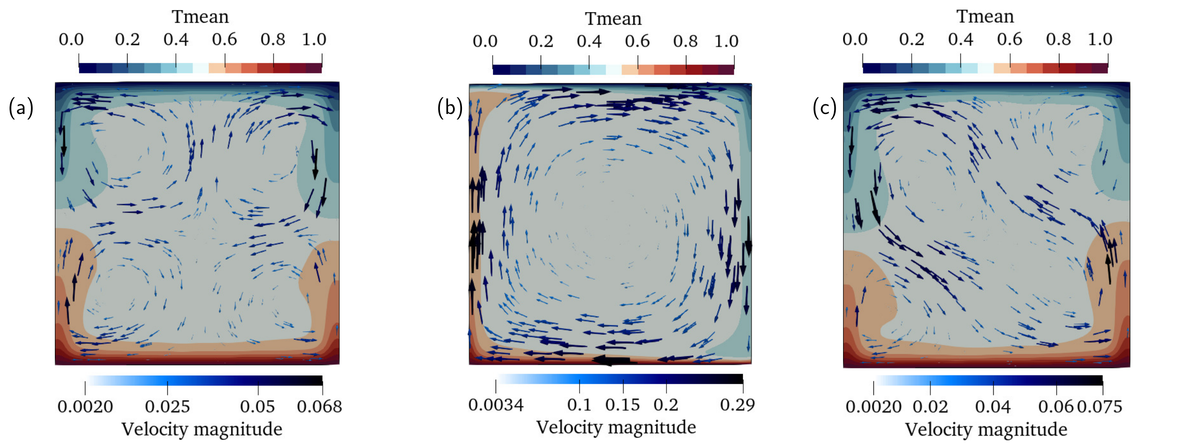

Figure 3: Time- and spanwise-averaged velocity flow patterns (arrows) and thermal distributions (color fields) for different boundary conditions: (a) No slip, (b) Free slip, (c) Finite slip.

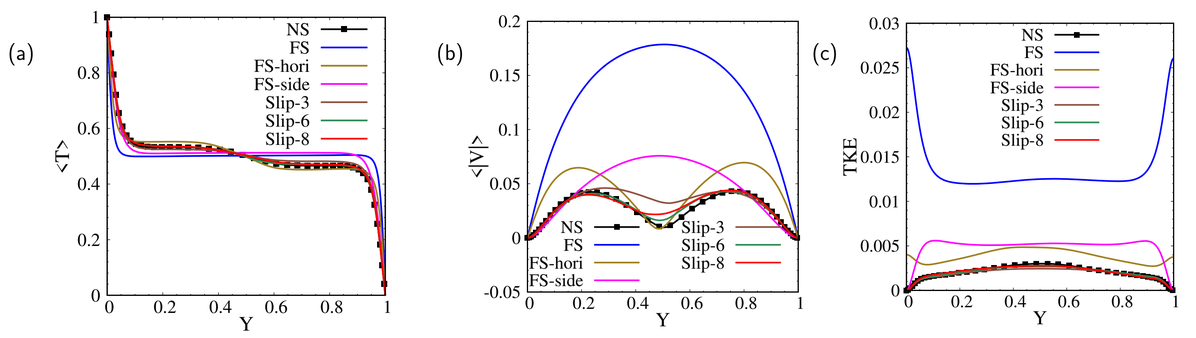

Figure 4: Horizontal-averaged profiles of (a) mean temperature, (b) mean vertical velocity, and (c) TKE along the cavity height.

(a)

Case	Nu	Case	Nu
NS	9.972	Slip-3	**10.425**
FS	**19.992**	Slip-4	9.904
FS-hori	**15.966**	Slip-5	10.217
FS-side	**11.141**	Slip-6	10.099
Slip-1	10.012	Slip-7	**10.448**
Slip-2	10.087	Slip-8	**9.682**

Table 1: Nusselt number obtained from the different boundary conditions simulations for $Ra = 2 \times 10^6$ and $Pr = 4.38$.

(b)

Ra	Pr	Walls	Nu
2×10^6		No-slip	10.27
2×10^6	0.786	Free-slip	**21.43**
2×10^6		Slip $l_s = 5 \times 10^{-4}$	10.30
2×10^6		No-slip	9.97
2×10^6	4.38	Free-slip	**19.99**
2×10^6		Slip $l_s = 5 \times 10^{-4}$	9.90
2×10^6		No-slip	9.81
2×10^6	10	Free-slip	**26.55**
2×10^6		Slip $l_s = 5 \times 10^{-4}$	9.75
1×10^7		No-slip	16.76
1×10^7	4.38	Slip $l_s = 1 \times 10^{-4}$	**17.27**
1×10^7		Slip $l_s = 5 \times 10^{-5}$	16.74

Table 2: Nusselt number obtained from the different boundary conditions simulations.

- **Fig. 5(a)–(c)** shows the difference in the attained turbulent flow states for different boundary conditions using the Lumley triangle analysis. In the case of no-slip and finite-slip wall boundaries, a multiple of turbulent states such as isotropic, axisymmetric state of one-component turbulence, and two-component axisymmetric turbulence states are observed when moving from the bottom wall to the top wall, whereas a dominant single-component axisymmetric turbulent state is presented in the free-slip case.

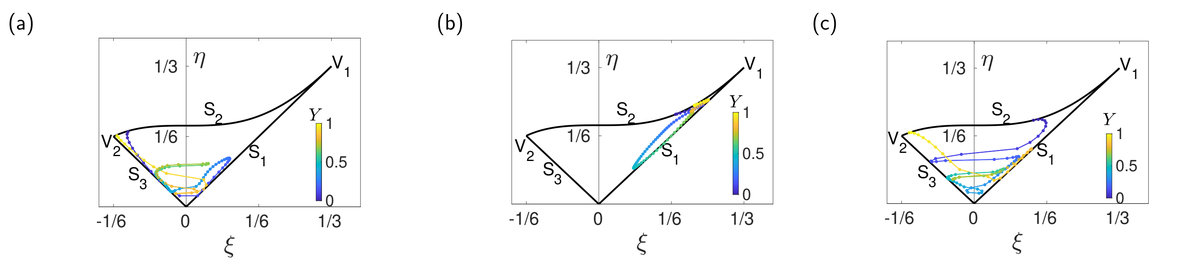

Figure 5: Lumley anisotropy analysis across the cavity. Pseudo color is used to indicate vertical location in terms of the normalized height coordinate Y = y/H (a) Case NS (b) Case FS (c) Case Slip-5.

Conclusions

- **Free-slip on all walls result in more than two times greater heat transfer compared to no-slip walls**, while also increasing velocity magnitudes and preventing flow reversal.
- Free-slip vertical walls strongly alter vortex structures. Free-slip horizontal walls enhance velocity magnitudes and heat transfer.
- Finite-slip conditions show minimal deviations from no-slip results, with only minor variations due to slip length or anisotropy at lower turbulent Rayleigh number.
- **Finite-slip walls yield heat transfer enhancement only for sufficiently vigorous turbulence at higher Rayleigh numbers.**

Acknowledgement

The authors gratefully acknowledge the computing time granted by the Resource Allocation Board and provided on the supercomputer Lise and Emmy at NHR@ZIB and NHR@Göttingen as part of the NHR infrastructure. The calculations for this research were conducted with computing resources under the project bbi00022.

This project is funded by the German government with funds from the Structural Development Act (Strukturstärkungsgesetz) for coal-mining regions and co-financed with funds from the state of Brandenburg.

LAND BRANDENBURG

With funding from the:

Federal Ministry of Research, Technology and Space

References

[1] C.-H. Choi, C.-J. Kim, *Physical Review Letters* **96**, 066001 (2006).

[2] D. Tritton, *Nature* **257**, 110 (1975).

[3] J. P. Rothstein, *Annual Review of Fluid Mechanics* **42**, 89 (2010).

[4] S. R. G. Polasanapalli, K. Anupindi, *Physics of Fluids* **34**, 035125 (2022).